

## HIGHLY EFFICIENT DRUG DELIVERY POLYMERIC MICELLES WITH CHARGE-SWITCHING AND CYCLIC RGD TARGETING FOR TREATMENT OF GLIOBLASTOMA

X. GUAN<sup>a,c</sup>, R. JIANG<sup>b</sup>, L. SUN<sup>b</sup>, W. CHEN<sup>b</sup>, H. TONG<sup>a</sup>, X. SUN<sup>a</sup>,  
K. FENG<sup>b</sup>, X. GAI<sup>c\*</sup>

<sup>a</sup>Research Center for Life Sciences, Beihua University, Jilin, China

<sup>b</sup>College of Chemistry and Biology, Beihua University, Jilin, China

<sup>c</sup>School of Basic Medical Sciences, Beihua University, Jilin, China

Efficient delivering anti-cancer drugs into tumor cells and significantly improving the intracellular drug concentration is a major challenge for cancer therapy. The enhanced permeability and retention effect (EPR) effect could improve the drug accumulation in tumor tissues. However, the poor cellular uptake of drugs still limits the efficacy of cancer chemotherapy. In this study, we developed an efficient drug delivery polymer micelles combining charge switching and cyclic RGD target. The negative charge of polymer micelles in physiological environment could switch to positive charge in tumor acidic environment mediated by imidazole. This charge switching property and RGD decoration collaboratively lead to significantly enhanced cellular uptake of drug-loaded micelles by glioblastoma cells.

(Received May 4, 2015; Accepted July 15, 2015)

*Keywords:* drug delivery; charge-switching; glioblastoma

### 1. Introduction

Glioblastoma is the most aggressive brain tumor in adults among human tumors which is characterized by the extensive network of abnormal vasculature. Due to the unrevealed mechanism of angiogenesis and origination of tumor endothelial cells, the median survival of most patients is generally less than two years from the time of diagnosis(1). Surgical resection, radiotherapy and chemotherapy represent three main effective treatments for glioblastoma(2). Although combination of several chemotherapeutic drugs proved to play a role in glioblastoma therapy, the severe side effects in clinical use impede its further application for cancer therapy(3). Efficient delivery of anti-cancer drugs into tumor cells and significantly improving the intracellular drug concentration is a major challenge for cancer therapy due to drug resistance and inefficient cellular uptake.

Progresses in nanomedicines during the past decade hold great promise for glioblastoma therapy(4,5). Nanomedicine used for cancer therapy is defined as anti-cancer drugs which are encapsulated or conjugated in nano-sized structures. Due to their nano size, nanomedicines offer several advantages over conventional chemotherapeutic drugs, such as improved solubility and bioavailability, reduced system toxicity, increased drug accumulation caused by enhanced permeability and retention effect (EPR) effect, and active targeting properties(6-8). Therefore, many types of nanomedicines have been developed to improve the efficacy of cancer therapy, and some of which had been approved for clinical use (for example, Doxil and Abraxane)(9-11). However, the EPR effect can only improve the drug accumulation in tumor stroma, the poor subsequent cellular uptake of anti-cancer drugs limit the efficacy of cancer chemotherapy.

To address this challenge, environment-responsive nanomedicines for cancer therapy had been designed and prepared by many researchers recently(12-14). These smart nanomedicines

---

\*Corresponding author: guanxg@ciac.ac.cn

nearly do not release the anti-cancer drugs in non-tumor tissues, but suggest fast drug release in tumors triggered by tumor microenvironment factors. Tumor microenvironment, which means various differences compared with normal tissue, include hypoxia, a decrease in pH, abnormal receptors and other characteristics(15,16). Among these factors, the low pH values in tumor areas is the most frequently used due to the dramatic contrast between tumor tissues and normal tissues(17-19). As is reported, the pH value in tumor tissues is much lower (6.5~7.4) than that in normal tissues (7.4)(20), and even more acidic environment (5.0~5.5)(21) can be detected in late endosomes and lysosomes. Until now a lot of pH-sensitive nanocarriers have been developed to enhance the delivery efficiency of anti-cancer drugs(22-24). These nanocarriers are stable under physiological conditions, and when pH values decreased to a trigger point these nanocarriers can rapidly release their payload to the acidic areas.

As a proof of concept, in this study we develop a nanocarrier with surface charge switching property for cancer therapy. The utilization of 1-(3-aminopropyl) imidazole (API) in the side chain of the polymer is capable of switch negative charge in physiological condition to positive charge in acidic environment via the protonation(25,26). As has been indicated by many researchers that the negatively charged cell membranes preferentially bind with the nanoparticles with positive charge, which directly lead to a higher internalization of positively charged nanoparticles(27). Moreover, to further improve the cellular uptake of nanomedicines, the nanocarriers were decorated with c(RGDfk) peptide whose receptor ( $\alpha_v\beta_3$  integrin) overexpressed in the plasma membrane of glioblastoma cells(28-31). The results indicated that our epirubicin (EPI) loaded pH-sensitive, cRGD decorated nanocarriers showed enhanced cellular uptake and improved cytotoxicity in C6 glioblastoma cells.

## 2 Experimental

### 2.1 Materials

c(RGDfk) peptide was customized from Shanghai China Peptides Ltd. Epirubicin (EPI) was purchased from Zhejiang Hisun Pharmaceutical Co. Ltd. Monomethoxy-poly(ethylene glycol) (MW=5000) was ordered from Aldrich. DAPI (4',6-diamidino-2-phenylindole) was purchased from Shanghai Yuanye Ltd., C6 glioblastoma cell was preserved in our own laboratory and cultured in Dulbecco's Modified Eagle Medium (Gibco) supplemented with 10% fetal bovine serum (FBS, Gibco).

### 2.2 Synthesis of mPEG-PCPGE-API

The methoxypoly(ethylene glycol) (mPEG)-block-poly[(2-carboxy-ethylsulfanyl)-propyl glycidyl ether] (PCPGE) was synthesized by our laboratory (32). Briefly, to introduce carboxyl groups, MPA was used to react with the mPEG-b-PAGE via thio-ene reaction. 0.2 g mPEG-b-PAGE (0.064 mmol) and 0.28 mL MPA (3.2 mmol) were dissolved in 20 mL of tetrahydrofuran in a 200mL round-bottomed quartz flask, then followed by degassing with N<sub>2</sub> for 30 min to eliminate the dissolved oxygen. The mixture was stirred at room temperature under UV light (254 nm, 1.29 mW/cm<sup>2</sup>) for 8 h. The mixture was concentrated in vacuo and poured into large amounts of cold diethyl ether to cause precipitation and to give the final product (yield=91%).

### 2.3 Synthesis of cRGD-PEG-PLA

The amphiphilic copolymer containing c(RGDfk) peptide cRGD-PEG-PLA was synthesized in our previous work(17).

### 2.4 Preparation of M(EPI) and RGD-M(EPI) micelles

M(EPI) micelles were prepared through solvent evaporation method. Briefly, 50 mg mPEG-PCPGE-API and 5 mg EPI was dissolved in 4 ml THF, and mix solution was added dropwise to 20 ml of deionized water. The suspension was stirred for 8 h at room temperature to remove the THF. This micelles were abbreviated as M(EPI). When M(EPI) micelles was used in

cellular uptake assay compared with RGD-M(EPI), these micelles were prepared using 50 mg polymer (mPEG-PCPGE-API: PEG<sub>5k</sub>-PLA<sub>3k</sub>=4:1, wt/wt) started.

Hybrid micelles RGD-M(EPI) were also prepared using the same method. 50 mg polymers (mPEG-PCPGE-API: cRGD-PEG<sub>5k</sub>-PLA<sub>3k</sub>=4:1, wt/wt) and 5 mg EPI were dissolved in 3 ml THF. The mixed solution was added dropwise to 10 ml of deionized water. The suspension was stirred vigorously for 8 h until no THF could be detected. The hybrid micelles RGD-M(EPI) composed of 20 wt% of cRGD-conjugated polymers, according to the content which had been proved to perform good tumor targeting ability (33,34). The morphology of EPI-loaded micelles was examined by transmission electron microscope (TEM) (JEOL JEM-1011 electron microscope). Size distribution of micelles was measured by dynamic light scattering (DLS) with a vertically polarized He-Ne laser (DAWN EOS, Wyatt Technologies). The scattering angle was fixed at 90° for DLS measurement at 25°C.

### 2.5 EPI release in vitro

The EPI release from M(EPI) and RGD-M(EPI) were examined using dialysis method at 37°C in PBS buffers (pH 5.8 and pH 7.4). For example, M(EPI) micelles containing 2 mg EPI was transferred into dialysis bag (MWCO=3000), which were immersed in 20 ml PBS buffer (50 mM, pH 5.8 and pH 7.4) with stirring at 100 rpm. At certain time points, 1 ml solution outside the dialysis bag was taken out for UV-Vis measurement (485 nm) and replenished with 1 ml fresh PBS solution.

### 2.6 Biocompatibility Assay

The biocompatibility of mPEG-PCPGE-API was investigated via MTT assay in C6 cells. Briefly, C6 glioblastoma cells were seeded in 96-well plates at a density of 3000 cells per well in 100 µL DMEM medium containing 10% fetal bovine serum (FBS). The second day the medium was discarded and replaced with 200 µL new medium containing different concentrations (ranging from 100 to 500 µg/mL) of blank micelles (prepared from mPEG-PCPGE-API, without EPI) for 48 h. After 48 h of incubation, 20 µL MTT (5 mg/mL in PBS buffer) was added to each well for 4 h incubation, finally 150 µL DMSO was added to dissolve the blue formazan, the absorbance was measured on a microplate reader (BioTek, EXL808) at 490 nm. This experiments were repeated three times.

### 2.7 Cellular uptake

The cellular uptake analysis of M(EPI) and RGD-M(EPI) micelles were investigated by confocal laser scanning microscopy (CLSM) and flow cytometry. Briefly, about  $3 \times 10^5$  C6 cells were seeded into each well of the six-well plate, and the second day the culture medium was replaced with fresh medium (EPI concentration: 5 µg/mL) for 1 h. The cells were washed with PBS for two times and fixed with 4% (w/v) paraformaldehyde for 10 min at room temperature. After washing with PBS, DAPI (6-diamidino-2-phenylindole) solution (5 µg/mL) was added to each well to label cell nuclei for 15 min. The images were captured via confocal microscope (Carl Zeiss LSM 780) under the same conditions. The average fluorescence intensity of each cell was measured by Image-Pro Plus (IPP) software under the same conditions.

### 2.8 In vitro cytotoxicity

The cytotoxicity of EPI-loaded micelles was evaluated via MTT assay in C6 cells. The processes of cell seeding and absorbance detection were same to that in biocompatibility assay except the drug adding. In this experiment, different concentrations (ranging from 0.01 to 10 µg/mL) of EPI or EPI-loaded micelles were added into each well for 48 incubation. The experiments were repeated three times.

### 2.9 Statistics

All experiments were performed at least three times and all results are expressed as mean±SD (standard deviation). Differences between groups were evaluated by analysis of student's t-test to demonstrate statistical significance ( $P < 0.05$ ).

### 3. Results and Discussion

#### 3.1 Synthesis of mPEG-PCPGE-API and RGD-PEG-PLA

In this study, the amphiphilic copolymer mPEG-PCPGE-API was synthesized through the amidation of mPEG-PCPGE with API in the presence of DCC/NHS (Fig.1).  $^1\text{H}$  NMR was used to characterize the chemical structure of mPEG-PCPGE-API. The result of  $^1\text{H}$  NMR (shown in Fig. 2) indicated that imidazole was successfully conjugated to the polymer of mPEG-PCPGE. The real content of API in mPEG-PCPGE-API is about 4.4:1 (the molar ratio of API to mPEG-PCPGE) calculated by the intensity of  $^1\text{H}$  NMR. The cRGD-PEG-PLA was synthesized in the literature, the molar ratio of cRGD to PEG-PLA was determined to 1:1.06 calculated by standard curve, which means that about 94% of polymer was conjugated with cRGD peptide.

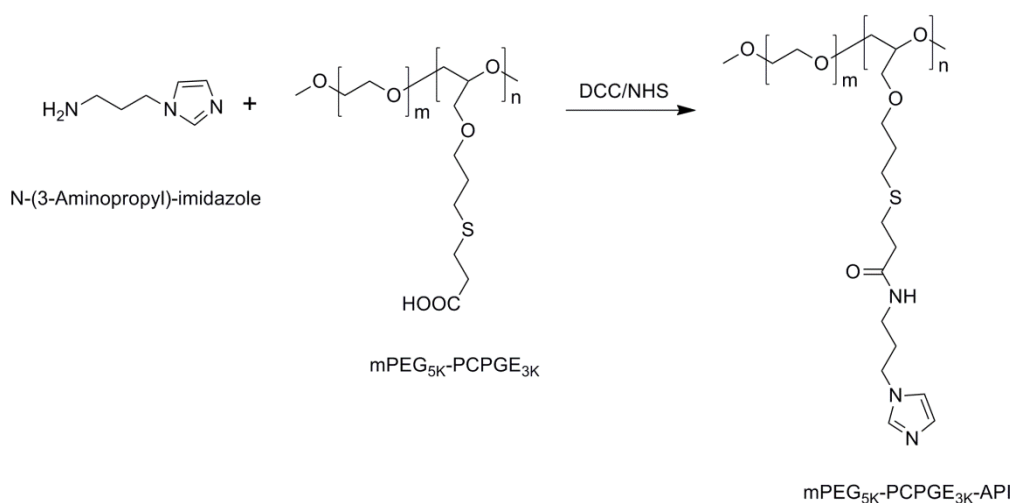


Fig. 1 Synthetic routes for preparation of mPEG-PCPGE-API.

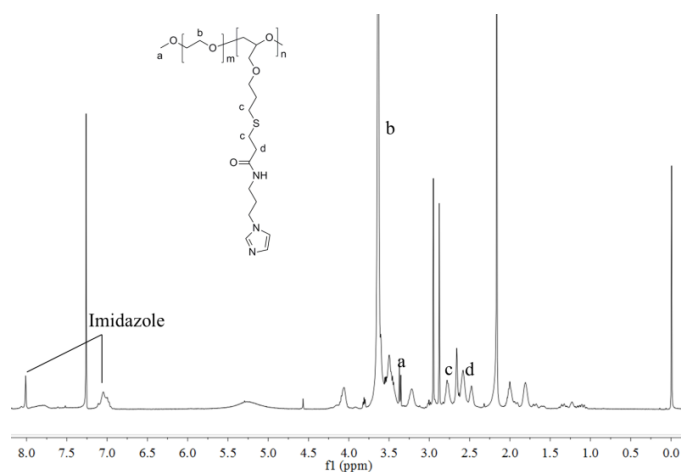


Fig. 2  $^1\text{H}$  NMR spectra of mPEG-PCPGE-API in  $\text{CDCl}_3$ .

#### 3.2 Preparation of M(EPI) and RGD-M(EPI) Micelles

In this study, solvent-evaporation method was used to prepare the EPI-loaded micelles. The result of TEM indicated that both M(EPI) and RGD-M(EPI) displayed nearly spherical morphology structure, and the mean sizes of two micelles were 63 nm and 70 nm respectively determined by DLS (Fig.3). The addition of RGD decoration on the surface of RGD-M(EPI) micelles may be responsible for their increasing size.

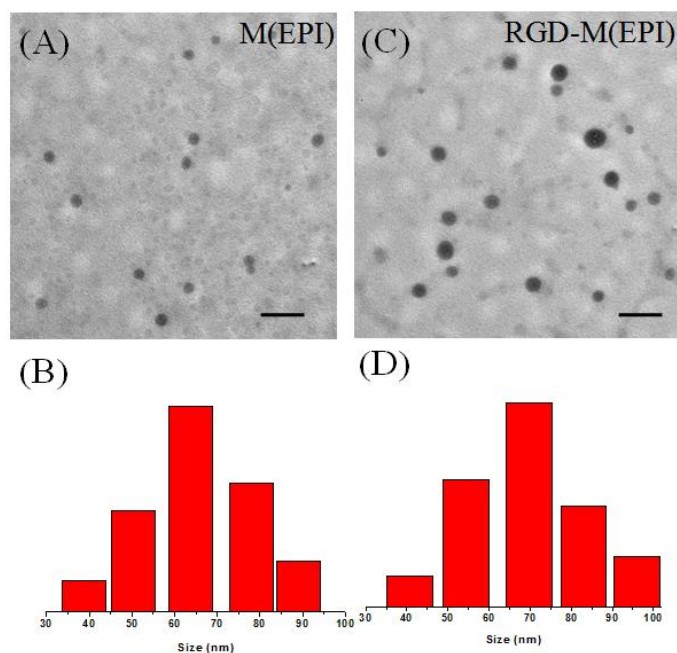


Fig. 3 Characterization of M(EPI) (A,B) and RGD-M(EPI) micelles (C,D) by DLS and TEM.

### 3.3 Drug release in vitro

The EPI release profile was evaluated by dialysis method. As shown in Fig.4, both M(EPI) and RGD-M(EPI) micelles displayed sustained release in different PBS buffer. After 48 h of release, the EPI cumulative releases of both micelles were merely released less than 30% in pH7.4 PBS, while the total release of two micelles increased to about 60% in acidic environment (pH5.8 PBS), suggesting a pH-responsive characteristic of our micelles.

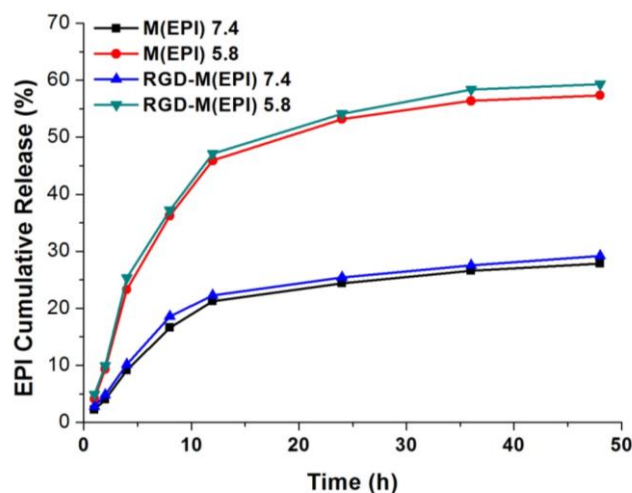


Fig. 4 EPI release profiles of M(EPI) and RGD-M(EPI) micelles in pH7.4 and pH5.8 PBS buffer.

### 3.4 Biocompatibility of mPEG-PCPGE-API polymers

To examine if our mPEG-PCPGE-API polymer could be used to prepare nanocarriers for drug delivery, the biocompatibility blank micelles prepared by mPEG-PCPGE-API was analyzed

via MTT assay. Different concentration of polymers (from 100 to 500  $\mu\text{g}/\text{mL}$ ) were used to test the cell viability. The results (shown in Fig.5) showed that cells displayed good cell viability at all tested concentration, and even at the concentration of 500  $\mu\text{g}/\text{mL}$  micelles the cell viability was still more than 87.5%, indicating good biocompatibility of our polymers.

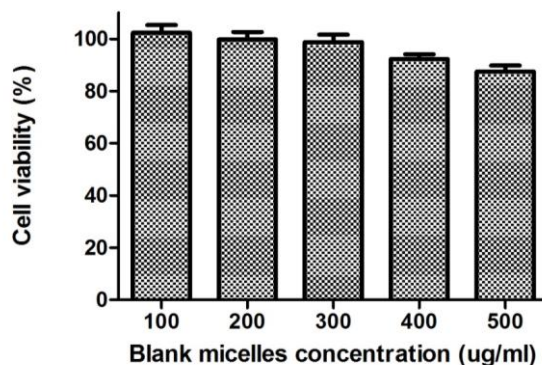
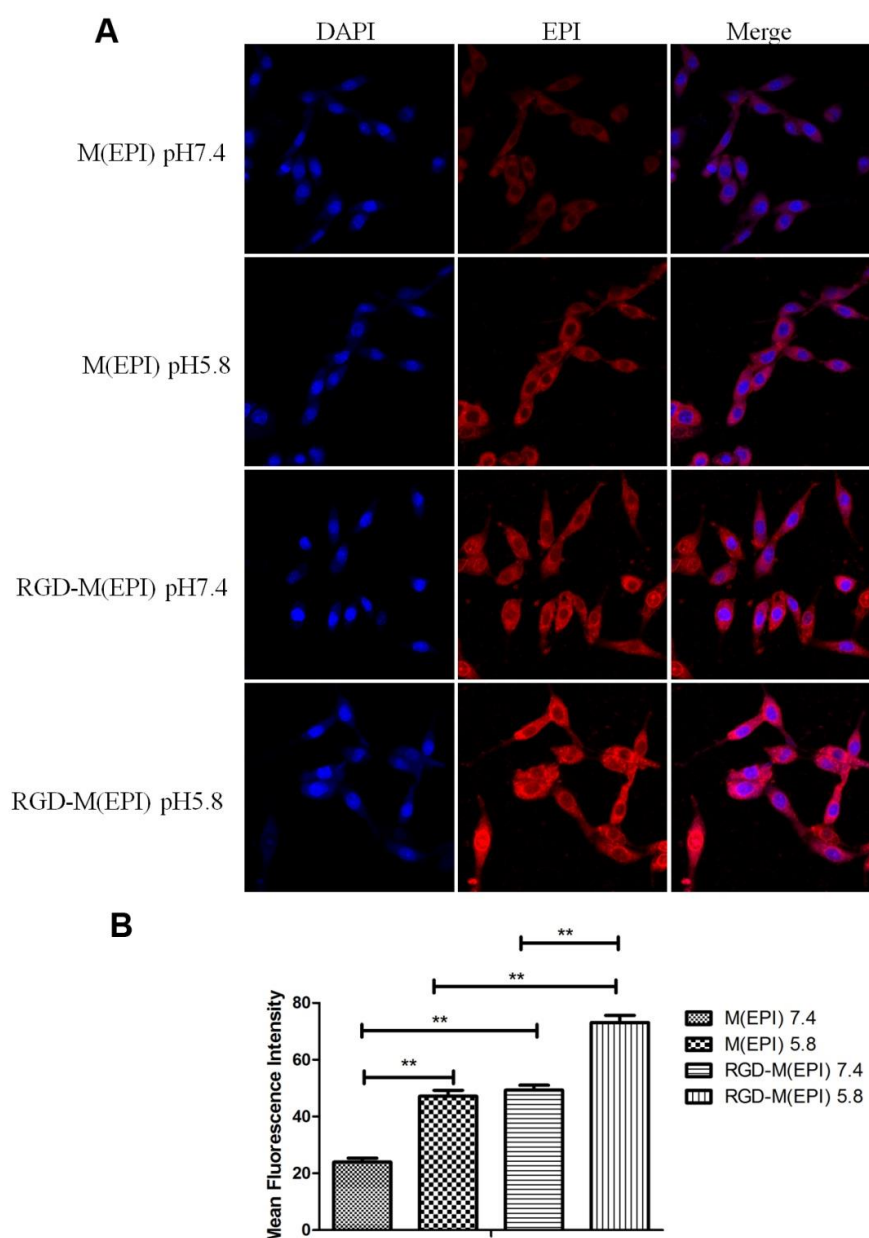


Fig. 5. Biocompatibility analysis of blank micelles prepared by mPEG-PCPGE-API. Cell viability of C6 cells treated with blank micelles at different concentration (from 100 to 500  $\mu\text{g}/\text{mL}$ ) after 48 h incubation at 37°C.

### 3.5 Cellular uptake

Based on the pH-responsive characteristic indicated by drug release experiment, we next performed cellular uptake analysis on C6 cells by CLSM imaging and flow cytometric experiment. The internalization of M(EPI) and RGD-M(EPI) micelles could be detected according to the inherent fluorescence of EPI. As shown in Fig. 6A, the red fluorescence was distributed in cytosol of C6 cells after 1 h of incubation, and the fluorescence intensity of M(EPI) in pH5.8 PBS buffer was much higher than that in pH7.4 PBS, which was confirmed by quantitative analysis by IPP software. The phenomenon was also observed in cells treated with RGD-M(EPI) micelles. The enhanced cellular uptake in acidic environment could be interpreted as the fast drug release caused by protonation of imidazole in hydrophobic core of micelles. When compared with M(EPI) micelles in the same PBS (pH7.4 or 5.8), cRGD-decorated micelles had more internalization in C6 cells indicated by Fig. 6A and 6B.



*Fig. 6 Cellular uptake analysis of M(EPI) and RGD-M(EPI) micelles in C6 cells by CLSM.*

*The cells were incubated with micelles for 1 h at pH 7.4 and pH 5.8 PBS at 37 °C(A); the mean fluorescence intensity of EPI of each cell were evaluated by IPP software (B).*

As reported by many researchers, there was high level of  $\alpha_v\beta_3$  integrin expression (the receptor of RGD domain) in the cell membrane of glioblastoma cells, and RGD-decorated nanoparticles could be quickly internalized into cells via receptor mediated endocytosis which was much faster than non-decorated. So this could be responsible for the increased internalization of RGD-M(EPI) micelles. The results of flow cytometric experiments (shown in Fig.7) were consistent with CLSM imaging. In acidic PBS, the cellular uptake rate of M(EPI) micelles raised to 68.9% which was 59% in pH7.4 PBS. As for RGD-decorated micelles, the rates of internalization were 74.3% and 87.5% in pH7.4 and pH5.8 PBS respectively. RGD-M(EPI) micelles in pH5.8 PBS showed the most cellular uptake in all groups, this was attributed to the synergy effect of RGD-decoration and pH-responsive characteristic in improving endocytosis.

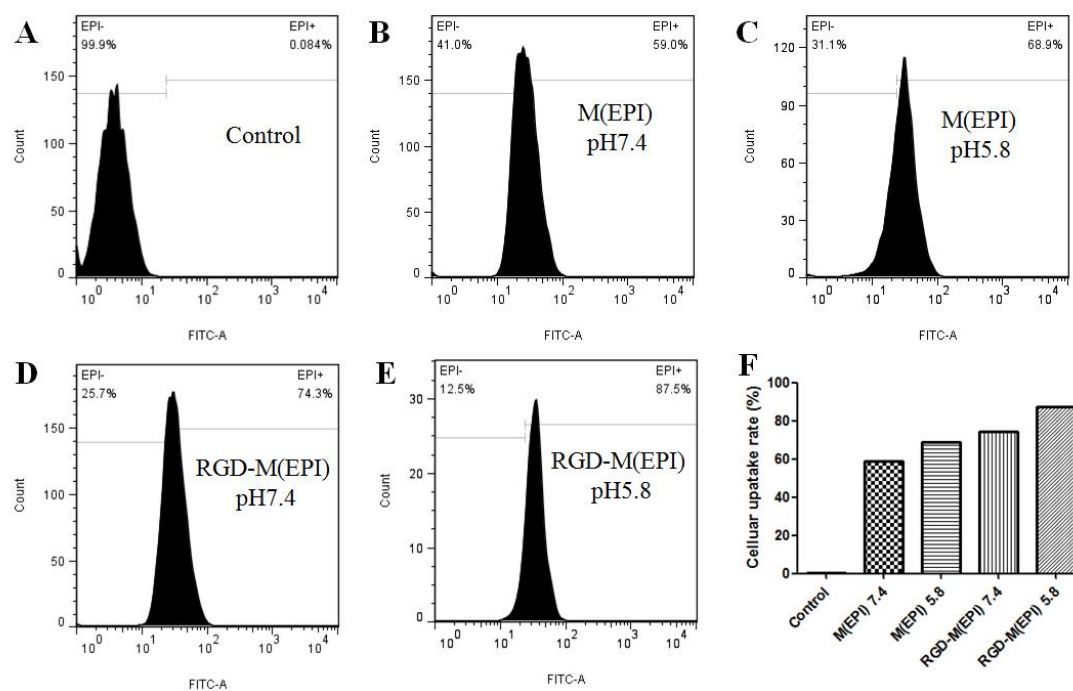


Fig. 7 Cellular uptake analysis of M(EPI) and RGD-M(EPI) micelles in C6 cells by flow cytometry analysis. Control (A); M(EPI) pH7.4 (B); M(EPI) pH5.8 (C); RGD-M(EPI) pH7.4 (D); RGD-M(EPI) pH5.8 (E); cell uptake rate of C6 cells (F).

### 3.6 Cytotoxicity analysis

Based on the data acquired by cellular uptake analysis, we evaluated the cytotoxicity of our micelles in C6 cells with free EPI as a positive control. The cell viability of C6 cells treated with free EPI, M(EPI) and RGD-M(EPI) for 48 h at the indicated concentration. The results (shown in Fig.8) showed that cell viability showed a dose-dependent manner for three types of EPI formulation. As is known that free EPI could transport into cells through free diffusion, therefore it showed the most cytotoxicity against C6 cells in three formulations. As for EPI-loaded micelles, RGD-M(EPI) micelles showed more cytotoxic than M(EPI). The higher cytotoxicity of RGD-decorated micelles was attributed to the more cellular uptake as indicated by CLSM and flow cytometric experiments, suggesting a good prospect of glioblastoma therapy.

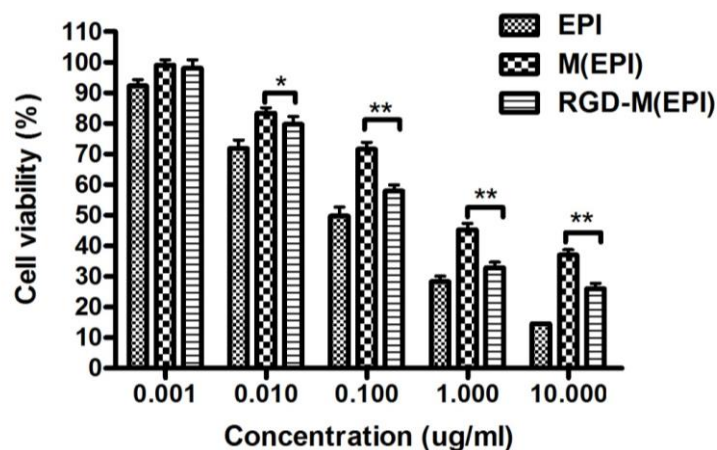


Fig. 8 The cytotoxicity analysis of C6 cells treated with M(EPI) and RGD-M(EPI) micelles for 48 h at 37 °C. All the results were repeated three times, and presented as mean  $\pm$ SD.

#### 4. Conclusions

In summary, dual functional EPI-loaded micelles decorated with cRGD peptide and imidazole were developed in this study. The polymer which was used to prepared drug delivery nanocarriers owns good biocompatibility, and EPI-loaded micelles shows a pH-responsive release profile in vitro. By combining the tumor targeting of cRGD decoration and pH-responsive property of imidazole, our micelles could significantly improve the cellular uptake of C6 glioblastoma cells indicated via CLSM and flow cytometric experiments. Furthermore, the cRGD decorated micelles also showed higher cytotoxicity to C6 cells than undecorated micelles. Our study indicated that cRGD decoration and imidazole own great advantage in improving cellular uptake of tumor cells, and could be used to design more efficient drug delivery system.

#### Acknowledgements

The project was supported by the Grant No. 20110728 and 20130522045JH from Science and Technology Department of Jilin Province, National Natural Science Foundation of China (Project No. 91227118 and 51373167), National Key Technology R&D Program (No.2012BAI29B05).

#### References

- [1] J. Clarke, N. Butowski, S. Chang, *Arch. Neurol-chicago*, **67**, 279 (2010).
- [2] R. Nishikawa, *Neurol. Med-chir.*, **50**, 713 (2010).
- [3] K. Maier-Hauff, F. Ulrich, D. Nestler, H. Niehoff, P. Wust, B. Thiesen, H. Orawa, V. Budach, A. Jordan, *J. Neuro-oncol.*, **103**, 317 (2011).
- [4] L. Agemy, D. Friedmann-Morvinski, V. R. Kotamraju, L. Roth, K. N. Sugahara, O. M. Girard, R. F. Mattrey, I. M. Verma, E., Ruoslahti, *Proc. Natl. Acad. Sci. U. S. A.*, **108**, 17450 (2011).
- [5] H. Xin, X. Sha, X. Jiang, W. Zhang, L. Chen, X. Fang, *Biomaterials*, **33**, 8167 (2012).
- [6] Y. Mi, J. Zhao, S.-S. Feng, *Nanomedicine (London, England)*, **8**, 1559 (2013).
- [7] E. Blanco, A. Hsiao, A. P. Mann, M. G. Landry, F. Meric Bernstam, M. Ferrari, *Cancer Sci.*, **102**, 1247 (2011).
- [8] D. Peer, J. M. Karp, S. Hong, O. C. Farokhzad, R. Margalit, R. Langer, *Nat. Nanotechnol.*, **2**, 751 (2007).
- [9] Y. Zhao, D. Y. Alakhova, J. O. Kim, T. K. Bronich, A. V. Kabanov, *J. Controlled Release*, **168**, 61 (2013).
- [10] J. H. Grossman, McNeil, S. E., *Phys. Today*, **65**, 38 (2012).
- [11] A. M. Maharramov, I. N. Alieva, G. D. Abbasova, M. Ramazanov, N. S., Nabiyeve M. R. Saboktakin, *Dig. J. Nanomater. Bios.*, **6**, 419 (2011).
- [12] S. Mura, J. Nicolas, P. Couvreur, *Nat. Mater.*, **12**, 991 (2013).
- [13] I., Cobo, M., Li, B. S., Sumerlin, S., Perrier, *Nat. Mater.*, advance online publication, 2 (2015).
- [14] X., Yao, L., Chen, X., Chen, C., He, H., Zheng, X., Chen, *Colloid Surface B*, **121**, 36 (2014).
- [15] O., Trédan, C. M., Galmarini, K., Patel, I. F., Tannock, *J. Natl. Cancer Inst.*, **99**, 1441 (2007).
- [16] F., Danhier, O., Feron, V., Preat, *J. Controlled Release*, **148**, 135 (2010).
- [17] X. Guan, X. Hu, S. Liu, Y. Huang, X. Jing, Z. Xie, *RSC Advances*, **4**, 55187 (2014).
- [18] Z. Xu, S. Liu, Y. Kang, M. Wang, *Nanoscale*, **7**, 5859 (2015).
- [19] S. Wang, L. Zhang, C. Dong, L. Su, H. Wang, J. Chang, *Chem. Commun.*, **51**, 406 (2015).
- [20] L. E. Gerweck, K., Seetharaman, *Cancer Res.*, **56**, 1194 (1996).
- [21] K. Miyata, N. Nishiyama, Kataoka, K., *Chem. Soc. Rev.*, **41**, 2562 (2012).
- [22] W. Chen, F. Meng, R., Cheng, Z., Zhong, *J. Controlled Release*, **142**, 40 (2010).
- [23] F. Meng, Y. Zhong, R., Cheng, C. Deng, Z. Zhong, *Nanomedicine*, **9**, 487 (2014).
- [24] L. Qiu, M. Qiao, Q. Chen, C., Tian, M., Long, M. Wang, Z. Li, W. Hu, G. Li, L. Cheng,

- L. Cheng, H. Hu, X. Zhao, Chen, D., *Biomaterials*, **35**, 9877 (2014).
- [25] X. Hu, X. Guan, J. Li, Q. Pei, M. Liu, Z. Xie, X. Jing, *Chem. Commun.*, **50**, 9188 (2014).
- [26] D. Ling, H. Xia, W. Park, M. J. Hackett, C. Song, K. Na, K. M. Hui, T. Hyeon, *Acs Nano*, **8**, 8027 (2014).
- [27] J. Z. Du, T. M. Sun, W. J. Song, J. Wu, J. Wang, *Angew. Chem. Int. Ed.*, **122**, 3703 (2010).
- [28] S. Kunjachan, R. Pola, F. Gremse, B. Theek, J. Ehling, D. Moeckel, B. Hermanns, Pechar, M., Ulbrich, K., Hennink, W. E., *Nano Lett.*, **14**, 972 (2014).
- [29] W. Song, Z. Tang, D. Zhang, Y. Zhang, H. Yu, M. Li, S. Lv, Sun, H., Deng, M., X. Chen, *Biomaterials*, **35**, 3005 (2014).
- [30] Z. Zhen, W. Tang, C. Guo, H. Chen, X. Lin, G. Liu, Fei, B., Chen, X., Xu, B., Xie, J., *ACS Nano*, **7**, 6988 (2013).
- [31] H. A. Kim, K. Nam, Kim, S. W., *Biomaterials*, **35**, 7543 (2014).
- [32] J. Li, X. Hu, M. Liu, J. Hou, Z. Xie, Y. Huang, X. Jing, *J. Appl. Polym. Sci.*, 131, (2014).
- [33] Y. Miura, T. Takenaka, K. Toh, S. Wu, Nishihara, H., Kano, M. R., Ino, Y., T. Nomoto, Y. Matsumoto, Koyama, H., *ACS nano*, **7**, 8583 (2013).
- [34] X. Guan, X. Guan, H. Tong, Ma, J., Sun, X., *J. Macromol. Sci. A*, **52**, 401 (2015).